LAWRENCE
LIVERMORE
NATIONAL
LABORATORY

UCRL-TR-228447

Bioforensics: Characterization of biological weapons agents by NanoSIMS

P.K. Weber, S. Ghosal, T.J. Leighton, K.E. Wheeler, I.D. Hutcheon

February 28, 2007

Disclaimer

This work performed under the auspices of the U.S. Department of Energy by Lawrence Livermore National Laboratory under Contract DE-AC52-07NA27344.

FY06 LDRD Final Report

Bioforensics: Characterization of biological weapons agents by NanoSIMS

LDRD Project Tracking Code: 04-ERD-039
Peter K. Weber, Principal Investigator

Abstract

The anthrax attacks of Fall 2001 highlight the need to develop forensic methods based on multiple identifiers to determine the origin of biological weapons agents. Genetic typing methods (i.e., DNA and RNA-based) provide one attribution technology, but genetic information alone is not usually sufficient to determine the provenance of the material. Non-genetic identifiers, including elemental and isotopic signatures, provide complementary information that can be used to identify the means, geographic location and date of production. Under LDRD funding, we have successfully developed the techniques necessary to perform bioforensic characterization with the NanoSIMS at the individual spore level. We have developed methods for elemental and isotopic characterization at the single spore scale. We have developed methods for analyzing spore sections to map elemental abundance within spores. We have developed rapid focused ion beam (FIB) sectioning techniques for spores to preserve elemental and structural integrity. And we have developed a high-resolution depth profiling method to characterize the elemental distribution in individual spores without sectioning. We used these newly developed methods to study the controls on elemental abundances in spores, characterize the elemental distribution of in spores, and to study elemental uptake by spores. Our work under this LDRD project attracted FBI and DHS funding for applied purposes.

Introduction/Background

The anthrax attacks of Fall 2001 highlight the need to develop forensic methods based on multiple identifiers to determine the origin of biological weapons agents. Genetic typing methods (i.e., DNA and RNA-based) provide one attribution technology, but genetic information alone is not usually sufficient to determine the provenance of the material. Non-genetic identifiers, including elemental and isotopic signatures, provide complementary information that can be used to identify the means, geographic location and date of production. The primary goals of an attribution assessment are to provide timely and accurate answers to two vital questions:

1. Who are the perpetrators?
2. What is the likelihood of follow-on attacks?

The answers to these questions are crucial to determining if a terrorist incident represents a threat to national security and also provide essential information to law enforcement and crisis management agencies. In this work, we address this national need by developing the capability to characterize biological weapons (BW) agents at the level of single cell and spore measurements using the unique capabilities of NanoSIMS (Fig 1).

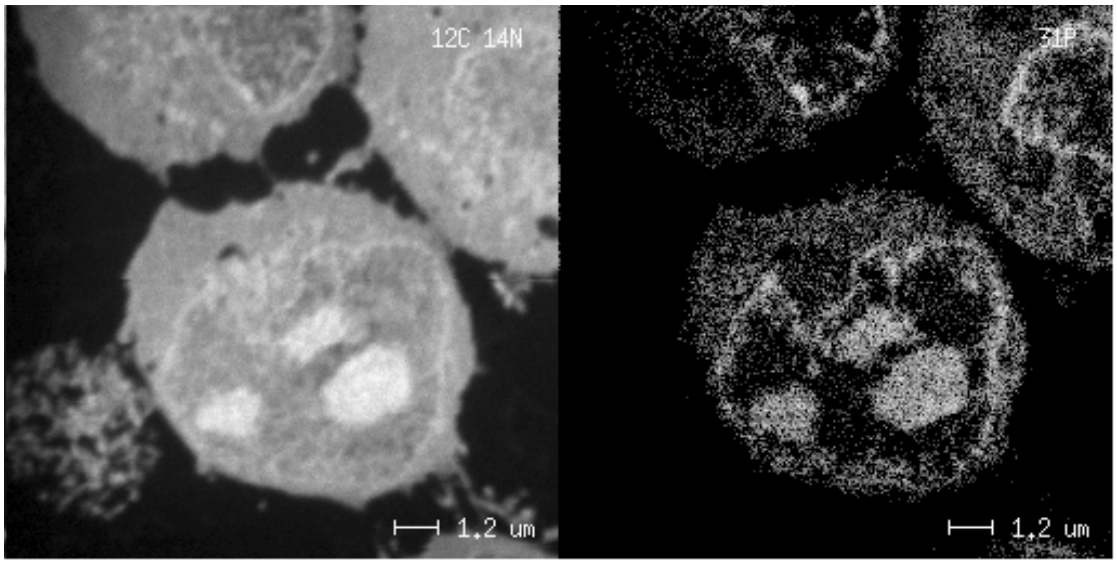

Fig. 1. LLNL NanoSIMS ion images of non-Hodgkin's lymphoma cells. The left panel shows the $^{12}C^{14}N$ image, and the right panel shows the ^{31}P image of the same set of cells. Cell components, including nucleus, nucleoli, and organelles are resolved. The images have ~50 nanometer resolution. Note 1.2 micron scale bars.

Potential signatures of spore production that can be measured by NanoSIMS are elemental composition, elemental distribution, and isotopic composition of the spores and the associated material in the sample. Spore isotopic composition is the most study of these signatures. The spore H, C, N and O isotopic compositions are determined by isotopic compositions of the media and water the spores are grown in (Hortia and Vass, 2003; Kreuzer-Martin et al., 2003).

The complexity of BW agents and the great variety in means of production, as well as the need to characterize evidentiary samples without fear of contaminants, requires a concerted new research effort. BW agents can be produced by a variety of different methods and with different mixtures of nutrients and additives. The spore material in itself is heterogeneous, with several layers with distinct chemical properties (Fig. 2). For example, the coat is composed of proteins with a high S content (~1% by weight), and the core is high in dipicolinic acid (5-15%) and Ca (4-8%). Furthermore, growth media residual on the spore surface is patchy. In addition to the microorganism, BW includes a matrix of weaponizing additives intended to enhance delivery, and forensic samples collected from certain environments will have considerable contamination from external material. Therefore, to develop elemental and isotopic signatures for attribution, it will be necessary to have high spatial resolution and sensitivity to analyze the bioagent particles on a sub-organismal level to account for spore and sample heterogeneity. An accurate

attribution assessment also requires the ability to selectively analyze individual bioagent particles (spore or stabilized cell) that may lie amongst environmental contaminants unrelated to the agent. Spore material is typical ~1 micron in diameter. To date, high spatial resolution (sub-micron) elemental analyses on spores have been limited to major elements. Measurements of trace element and isotopic ratios have been performed by bulk analyses (e.g., Hortia and Vass, 2003; Kreuzer-Martin et al., 2003).

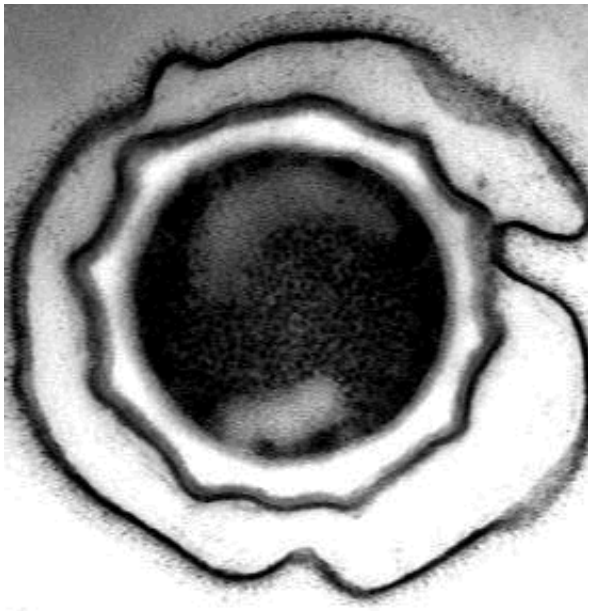

Fig. 2. Transmission electron microscopic view of a *B. cereus* spore ultrathin cross section. The electron dense central spore core is overlaid by: the electron transparent spore cortex; a moderately electron dense inner spore coat layer; an opposed electron dense outer spore coat layer; and the loosely associated exosporium layer. Note the presence of filamentous appendages projecting from the surface of the exosporium. Image width: 1 micron. (Source: T. Leighton, CHORI)

The ability of the NanoSIMS to characterize the substructure of spores is a key feature of this research. One of the fundamental characteristics of spores is that they are elementally zoned at the nanometer scale. The most readily observed elemental zonation is the high Ca content of the core, which corresponds with the presence of dipicolinic acid. This zonation provides a template against which to compare the distribution of other elements in spores. Spore elemental zonation may be a function of biological factors, physical factors, and elemental diffusion. Of these factors, only biological factors have previously been documented, as in the case of calcium and phosphorus being more abundant in the core, and sulfur being more abundant in the coat because of disulfide cross-linking. Elements that are known to substitute for biologically localized elements, such as Sr substituting for Ca, are expected to be similarly located. We hypothesize that physical factors such as hydration/dehydration control the initial distribution of elements such as chlorine and fluorine, which are typically observed on the spore margin, but this idea is yet to be tested. Similarly, the control on mineral layers on the spore coat is not known. Variations from the typically observed elemental zonation may result from changes in production factors that affect these biological and physical factors.

Spores are known to be permeable to water and small molecules (Gerhardt & Black, 1961; Westphal et al., 2003). Therefore we expect that movement of elements in and out of spores will play an important role in elemental distribution and abundance. Elemental redistribution will occur when elemental distributions are out of thermodynamic equilibrium, such as during washing of spores. The produced spores can

also be out of internal equilibrium, or they can be placed into a disequilibrium state as the result of exposure to external elemental gradients after production. Our expectation is that ion mobility will be very slow under dry conditions, rapid under fully hydrated conditions, and moderate at ambient humidity conditions, but this idea is yet to be tested.

STEM has been used to map the elemental zonation of spores with very high spatial resolution (<10 nm). This technique is very effective for major and minor elements (>0.1% by mass). Its sensitivity, however, is not sufficient for studying trace elements, and it cannot be used for making isotopic measurements. Here we use nanometer-scale secondary ion mass spectrometry (NanoSIMS), which allows trace elemental characterization (ppm by weight) with high spatial resolution (~10 nm depth and 50 nm lateral). NanoSIMS also allows quantitative total elemental and isotopic characterization of trace samples. The NanoSIMS methods that we developed allow us to collect baseline data elemental gradients in spores, for the variability in elemental abundance within and between samples, and for diffusion within spores.

Research Activities

We used NanoSIMS to characterize spores. NanoSIMS is the latest advance in secondary ion mass spectrometry (SIMS), an in-situ method of mass spectrometry whereby secondary ions from the sample are produced by sputtering with a primary ion beam and are entrained into the secondary mass spectrometer for analysis. NanoSIMS has 50 nm lateral resolution (Fig. 1) and 40 to 100X higher sensitivity than conventional SIMS instruments (useful yield approaching 10%). The NanoSIMS has a suite of five detectors for simultaneous collection of secondary ions, which enables precise and efficient measurements in small samples that are heterogeneous or consumed during the course of analysis. The primary ion beam can be rastered to construct secondary ion images of the sample. The NanoSIMS has two primary ion beams, Cs^+ and O^-. The Cs^+ primary ion beam enhances the yield of electronegative elements and in this study is used to analyze samples for C, N, F, Si, P, S and Cl. The O^- primary ion beam enhances the yield of electropositive elements and in this study is used to analyze samples for C, Li, Mg, Na, Si, Ca, Mn, Fe and Cs. C and Si were analyzed in both modes. The lateral spatial resolution of the secondary ion images is controlled by the primary beam spot size. The Cs^+ primary ion beam can be focused down to 50 nm, and the O^- primary ion beam can be focused down to ~150 nm. Depth resolution is controlled by the mixing depth of the primary ion beam, which is less than 10 nm for both Cs^+ and O^-.

Typically, we analyzed sectioned samples with a Cs^+ primary ion beam to determine elemental distributions. The samples were sectioned by focused ion beam (FIB) because we found that embedding for cryo or room-temperature ultramicrotomy resulted in elemental loss. Depth profiling was performed on whole spores to reduce preparation time, and in the case of O^- analyses, to increase spatial resolution.

We determined the elemental distribution in *Bacillus thuringiensis israelensis* (*Bti*) spores produced by T. Leighton and K. Wheeler of Children's Hospital Oakland Research Institute (CHORI). They produced reference samples and altered the elemental composition of the media in which the spores were grown to allow the characterization of the response in spores.

Diffusion experiments were carried out with dry and hydrated *Bti* spores from CHORI. Spores were first exposed to D_2O to characterize the rate of water uptake. To

study elemental uptake, spore aliquots added to dilute solutions of lithium fluoride and cesium chloride. Cation choices were based on the observation that Li and Cs have low abundance in spores and provide a range of ionic radii. After exposure, the samples were rinsed in milli-Q water three times (~5 minutes) and deposited on a substrate for drying in argon. Leach experiments were conducting by placing spore aliquots in milli-Q water, and then depositing the samples on a substrate for drying. The spores were analyzed by NanoSIMS depth profile method.

Data processing

The NanoSIMS generates quantitative ion images. Multiple images are taken successively to determine the evolution of the ion signal with time and enable better quantification. We have custom software that allows us to define regions of interest from which the data is extracted, such as the center of the spore.

Results/Technical Outcome

Sample preparation for NanoSIMS imaging

NanoSIMS imaging of spore substructure requires sectioning of the sample to expose the internal structure. We used three methods to produce sectioned spores: ultramicrotomy for resin embedded spores (Fig. 3), cryo-ultramicrotomy for frozen spores (Fig. 4), and focused ion beam (FIB) for untreated spores (Fig. 5). These sections were made as thin as 100 nanometers, making them electron transparent and allowing correlated TEM/STEM and NanoSIMS analyses. Electron transparent sections of spores were successfully imaged in the NanoSIMS (Figs. 3 & 5).

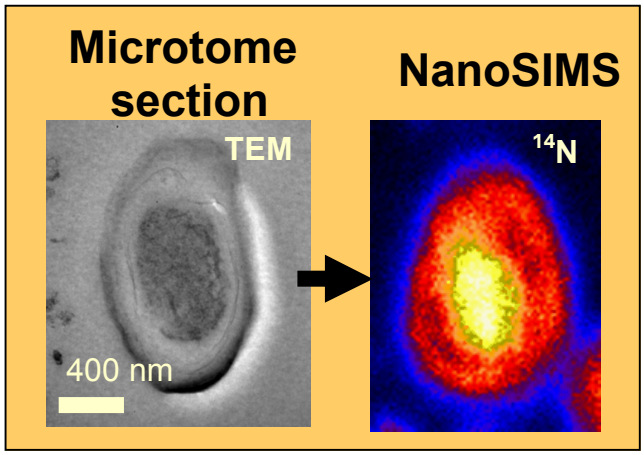

Fig. 3. Resin-embedded ultramicrotome section of a *Bti* spore and a NanoSIMS N ion image of a similar spore. TEM = transmission electron microscopy.

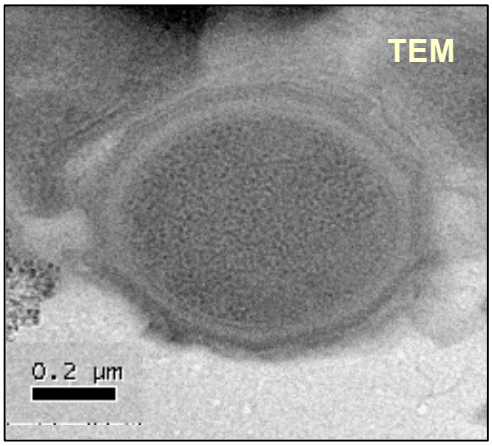

Fig. 4. Cryo-microtome section of a *Bti* spore produced at LLNL, showing the exosporium, coat and core. TEM = transmission electron microscopy.

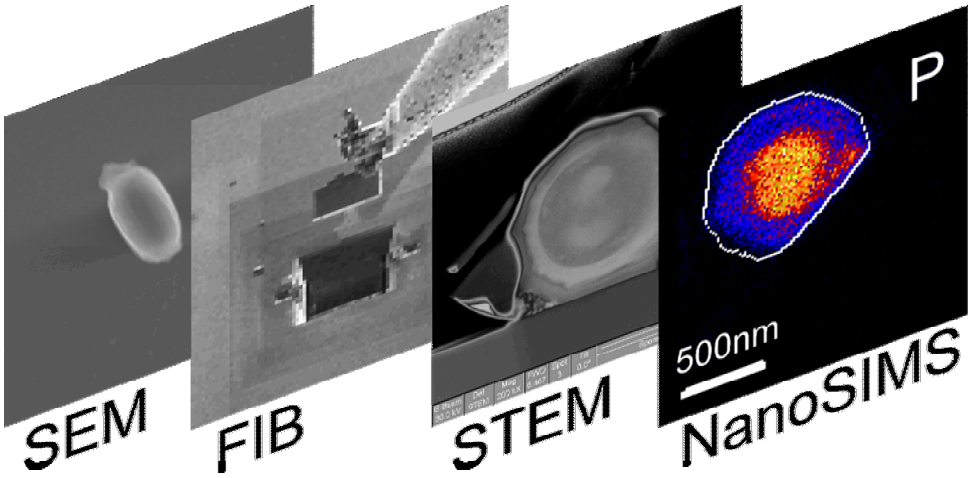

Fig. 5. Combined EM-FIB-NanoSIMS analytical sequence for a bacterial spore: SEM imaging, FIB sectioning and lift-out, TEM/STEM imaging, and NanoSIMS analysis.

While the ultramicrotomy methods work for sectioning spores and introduction into the NanoSIMS, we found that the embedding methods necessary for room temperature and cryo-ultramicrotomy have the potential to significantly alter the elemental composition of the sample. Immersing spores in water can result in elemental loss, including F and Si loss (Fig. 6). Therefore, we focused on FIB for sample sectioning.

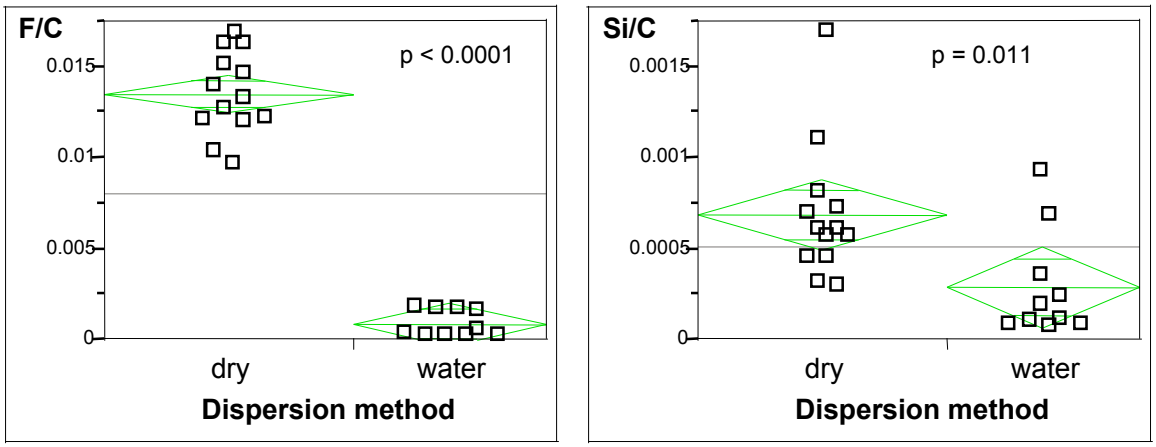

Fig. 6. Affect of exposure to liquids on spore elemental composition.

Standard FIB sectioning is slow because it requires precision thinning of the sample and careful manipulation of the sample to position it for analysis (Fig. 5). For NanoSIMS analyses alone, this full procedure is unnecessary. To speed up the process, we used the LLNL FIB to develop a new top-cut method for sectioning spores (Fig. 7). Spores are dispersed on a flat, conducting substrate, which is tilted so that the FIB beam hits the substrate surface at a glancing angle of ~10 degrees. The FIB top-cut removes the upper third to one-half of the spore to expose the core of the spore. This approach can produce approximately 20 spores suitable for NanoSIMS imaging in 4 hours.

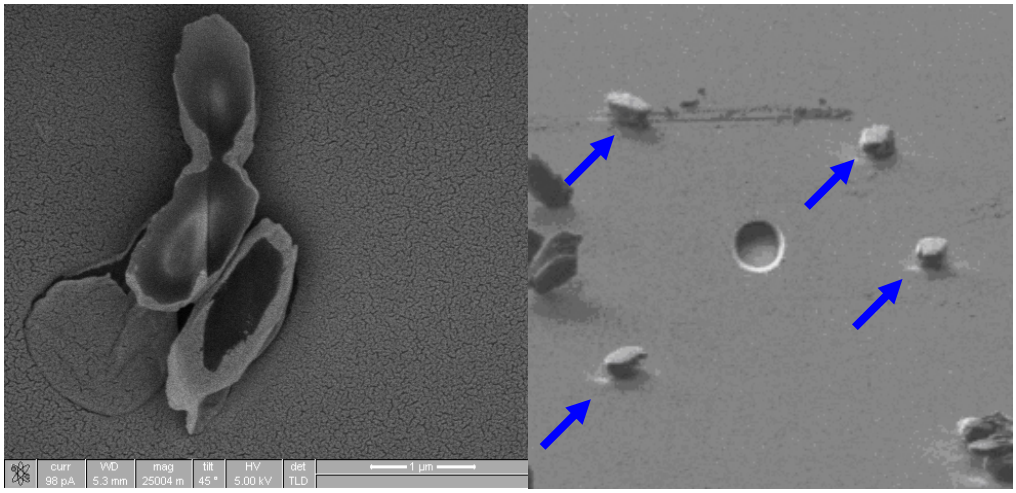

Fig. 7. Normal and oblique views of FIB top-cut *Bti* spores performed at LLNL. The left image shows that the core of the central spore was well exposed. The right image shows a fiducial mark (central circle) used to relocate the indicated top-cut spores.

Elemental Distributions

NanoSIMS images of FIB-sectioned spores show the expected distribution of biologically controlled elements (Fig. 8). Phosphorus levels are higher in the core, where DNA and ADP are located. Sulfur levels are highest in the coat because of disulfide cross linking. Carbon and nitrogen are throughout the spores (not pictured). These data demonstrate that FIB sectioning does not significantly alter the elemental distribution in spores, and that the NanoSIMS can extract these data. Such biologically controlled elemental distributions can be used as a quality control check for microanalysis. We regularly collect phosphorous data from spores when collecting negative secondary ions and see the same distribution.

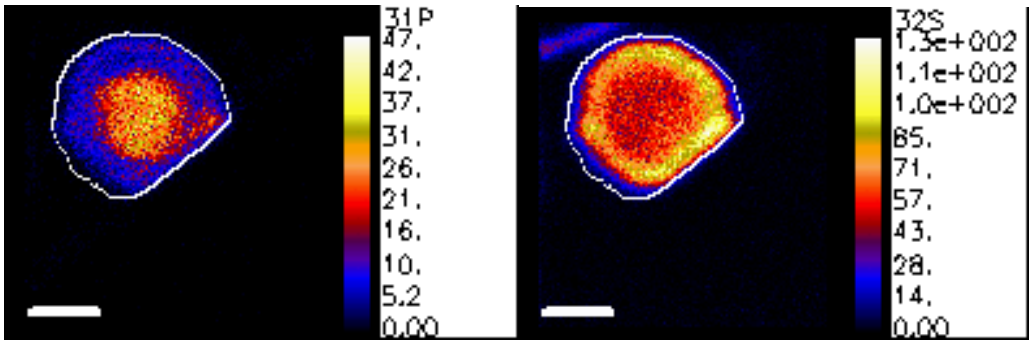

Fig. 8. P and S images of a FIB section of a *Bti* spore. Note high P in core and high S in coat layer, as expected based on spore structure. Scale bar = 500 nm.

Elements that we expect to be controlled by the physical processes of hydration/dehydration are typically found on the spore margin. Chlorine in particular is strongly associated with the spore margin (Fig. 9), with rare exceptions. Fluorine is also typically found at higher levels on the spore margin than in the core, but with more exceptions, such as show in Figure 9. Si is collocated with Cl.

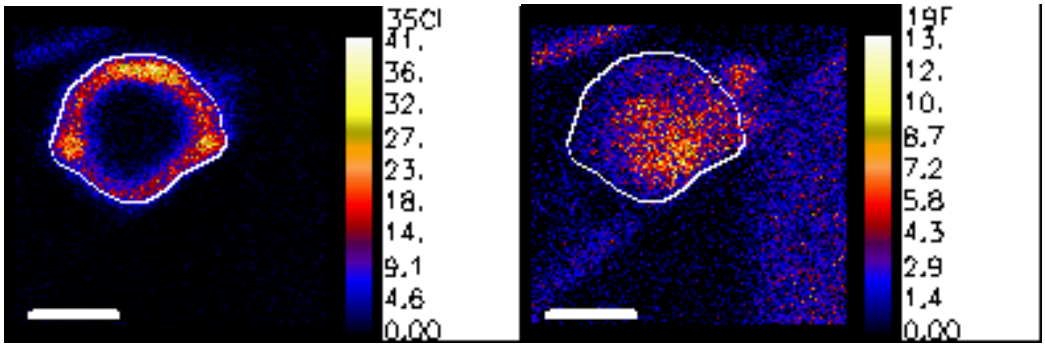

Fig. 9. Cl and F images of a FIB section of a *Bti* spore, showing anti-correlation. Typically, F is collocated with Cl.

Single spore depth profiling

After establishing the baseline elemental distribution within bacterial spores, we proceeded to determining if these distributions could be extracted from spores by depth profiling spores dispersed on a conducting substrate (e.g., Si wafer or Au foil). Depth profiling is a sample characterization method in which ions are collected from a sample while digging down into the sample. The value of the data is determined by the ability to resolve layers in the sample based on the depth profile data.

To evaluate the baseline ability of the NanoSIMS to perform depth profiles, we performed depth profiles with the NanoSIMS on a Si-C multilayer sample with 3 nanometer thick C layers and 25 nanometer thick Si layers using both the Cs^+ and O^- primary beams (Fig. 10). The data demonstrate that the NanoSIMS has better than 3 nanometer depth resolution for Cs^+, and approximately 10 nanometer depth resolution for O^-. Changes in ion yields at interfaces and degradation of sample structure due to sample mixing caused by primary ion implantation can further degrade the quality of the data...

Spores erode under SIMS ion beam sputtering in an anisotropic fashion (Fig. 11) because they are oblong spheroids with radially symmetric internal structure (Figs. 2, 3 & 4). Nonetheless, reasonable depth profiles of structure can be extracted for individual spores (Fig. 12). The carbon signal is relatively constant while depth profiling into the spore, and the spore can be edge can be set based on when the C signal falls below 50% of the maximum. Phosphorous intensity reaches a maximum after carbon, reflecting the P in the core of the spore. The core can be defined as the region within which the P signal is above 50% of the maximum P signal. Chlorine and silicon are most abundant at the spore margins, as seen in the NanoSIMS images, and fluorine is more variable.

Experimentation with depth profiling suggests that the outer layer is eroded away across the entire surface of the spore exposed to the beam, exposing the interior of the spore to the ion beam with only a small portion of the outer layers contributing to the ion signal, and then finally, the interior is eroded away, exposing the basal outer layers of the spore to ion beam sputtering. Depth profile quality is primarily affected by the primary ion beam species. The Cs^+ primary beam generates better depth profiles than the O^- primary beam, probably because the sputtering rate is higher and the depth resolution is better. Extracting the data from the central the central region of the spore can also improve quality for Cs^+ depth profiles, but is less important for O^- depth profiles.

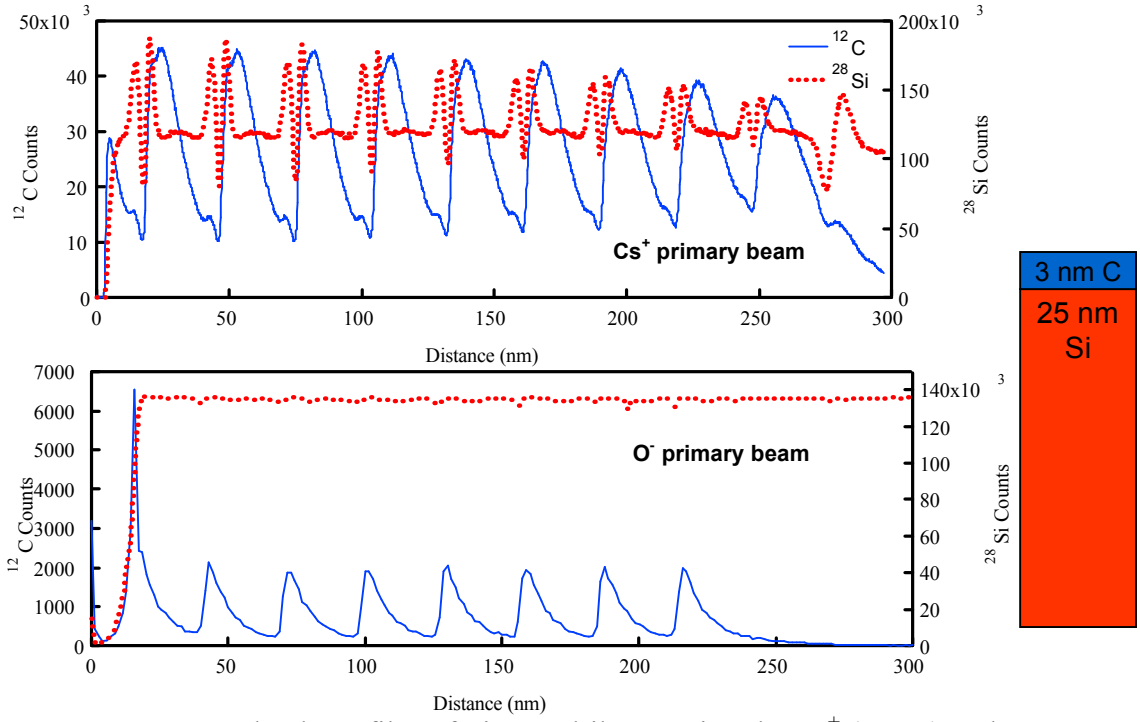

Fig. 10. NanoSIMS depth profiles of Si-C multilayer using the Cs^+ (upper) and O^- (lower) primary beams. A single multilayer subunit is represented on the right. The multilayer sample was comprised of 10 subuinits on a Si substrate.

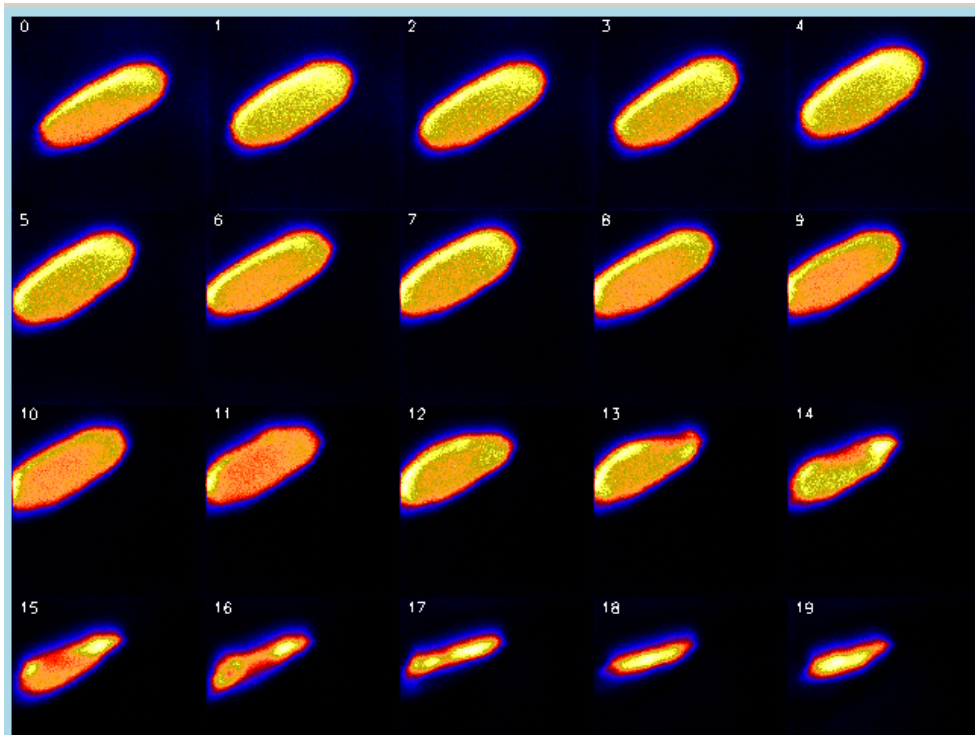

Fig. 11. Sequential NanoSIMS carbon ion images of a single spore being sputtered to exhaustion with a Cs^+ primary ion beam.

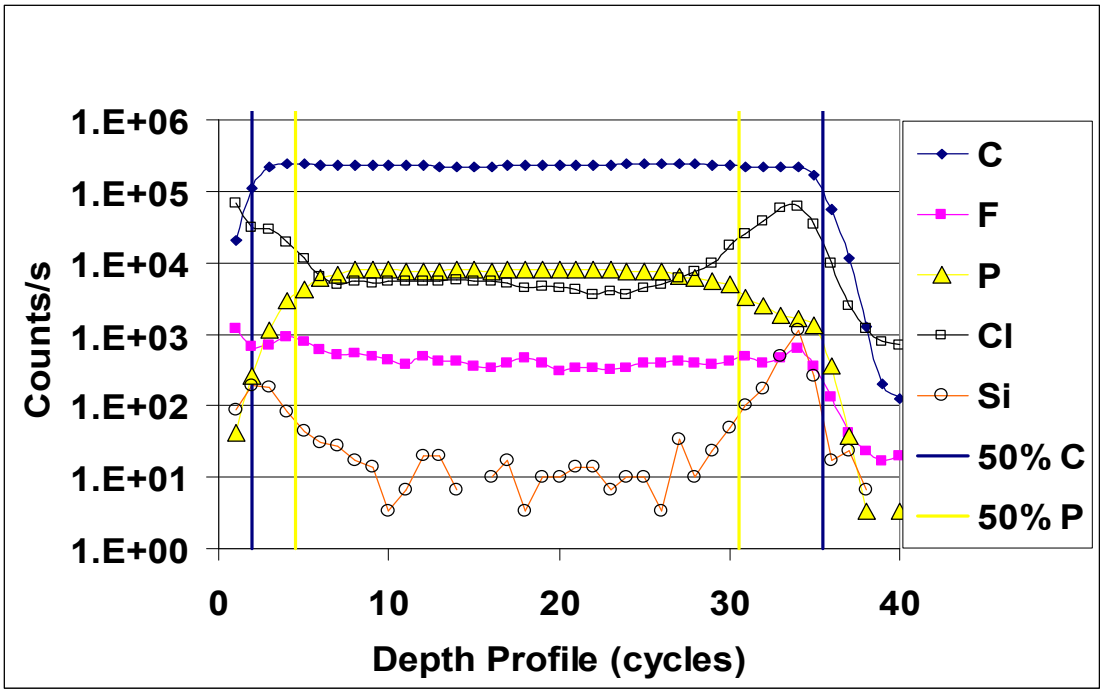

Fig. 12. NanoSIMS depth profile of a *Bti* spore, starting at the surface of the spore (cycle 1) until exhaustion (~cycle 40).

Isotopic characterization of spores

To make isotopic measurements, multiple spores must be analyzed to collect enough counts to have sufficient precision to differentiate samples based on isotopic composition. As part of this project we determined the limit of measurement precision based on the number of atoms collected for a given species from a single spore in the NanoSIMS. The data show that $^{13}C/^{12}C$ and $^{34}S/^{32}S$ ratios can potentially be measured to useful levels of precision with less than 10 spores. Other isotopic ratios of interest would require 10s to 100s of spores.

Isotopic Ratio	Range in growth media	Limit of precision for measurement with a single spore	Number of spore analyses to achieve $2\sigma = 1/10^{th}$ of growth media range
	(‰)	(2σ ‰)	(#)
$^{13}C/^{12}C$	15	3	5
$^{2}H/^{1}H$	75	130	306
$^{18}O/^{16}O$	20	12	36
$^{15}N/^{14}N$	5	4	56
$^{34}S/^{32}S$	20	6	9

Table 1. Comparison of limit of precision for selected isotopic ratio measurements, based on species counts from single spore measurements in the NanoSIMS.

Baseline controls on trace elements in spores

We performed elemental addition experiments with Sr and Ba to determine the response of spores to increase availability of these trace elements. We added Sr and Ba to the sporulation medium at 1, 10 and 100 micromolar levels and analyzed the spores by NanoSIMS. We found a direct positive relationship between the amount of each element

added and the concentration in the spore (Fig. 13). These experiments demonstrated that for elements that are not physiologically necessary and therefore regulated the elemental composition of the spore preparation can be directly related the medium used to produce the spores. Sr and Ba are chemically similar to Ca, and therefore should substitute for Ca in the core.

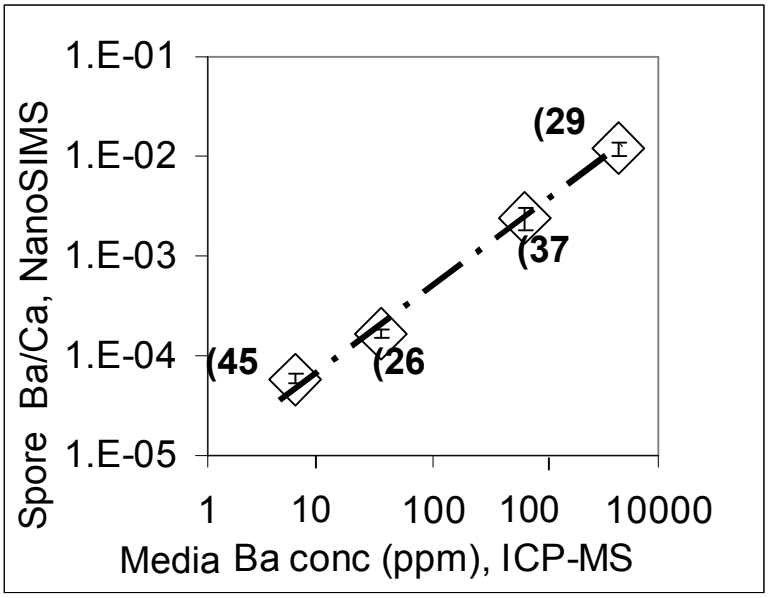

Fig 13. Response of spores to the Ba concentration in the media. Media analyses were made by ICP-MS, ans spore analyses were made by NanoSIMS.

Water and elemental uptake

Using deuterated water (D_2O), we demonstrated that water is taken up by spores and either retained or exchanged with water in the spore (Fig. 14). D_2O was detected in the core of spores exposed for less than 1 minute to D_2O vapor, showing that spores are highly permeable to water. The 50% saturation level is reached within an hour. The uptake of water by spores is in agreement with microscopy based measurement which found that spores swell when exposed to water, including water vapor at sub-saturation levels (e.g., ambient humidity) (Westphal et al., 2003). The time scale the NanoSIMS data reflects the rate of D_2O exchange with spore water and H. We hypothesize that water uptake will increase ion mobility in spores and that the resulting diffusion can be used to date the spores. This method would potentially be a high resolution method (less than 1 year) that would constrain the minimum age for a sample. This method would be complementary to carbon-14 dating, which sets the maximum age of a sample based on the date when the carbon used to produce the spores was fixed via photosynthesis.

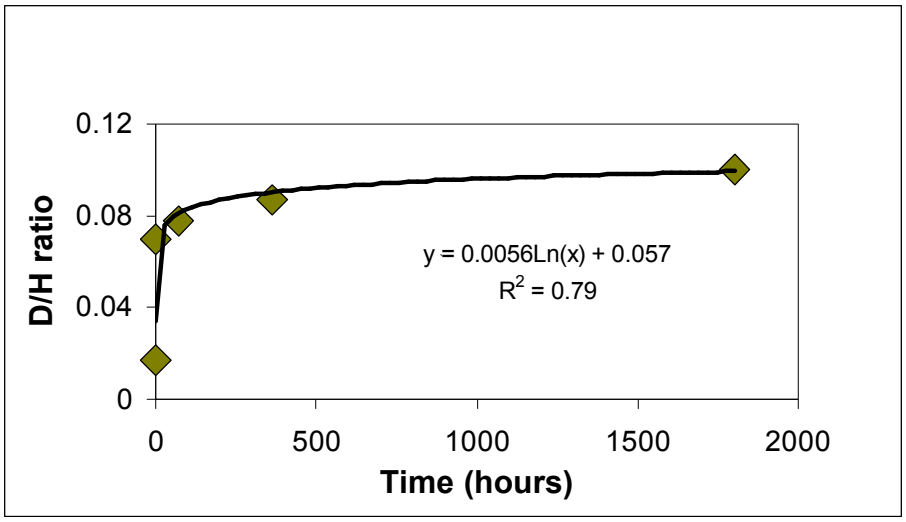

Fig. 14. Uptake of D_2O by *Bti* spores over time.

In our first elemental uptake experiments, we immersed dry spores in solutions with high LiF concentrations. The NanoSIMS data demonstrate diffusion of Li and F into the spore core in less than three days using a concentrated LiF solution (Fig. 15). Li content of the spore increased by more than 3 orders of magnitude over the control. Based on this result, we determined that we could work with dilute LiF solutions and still obtain sufficient signal for time step comparison and elemental profile characterization.

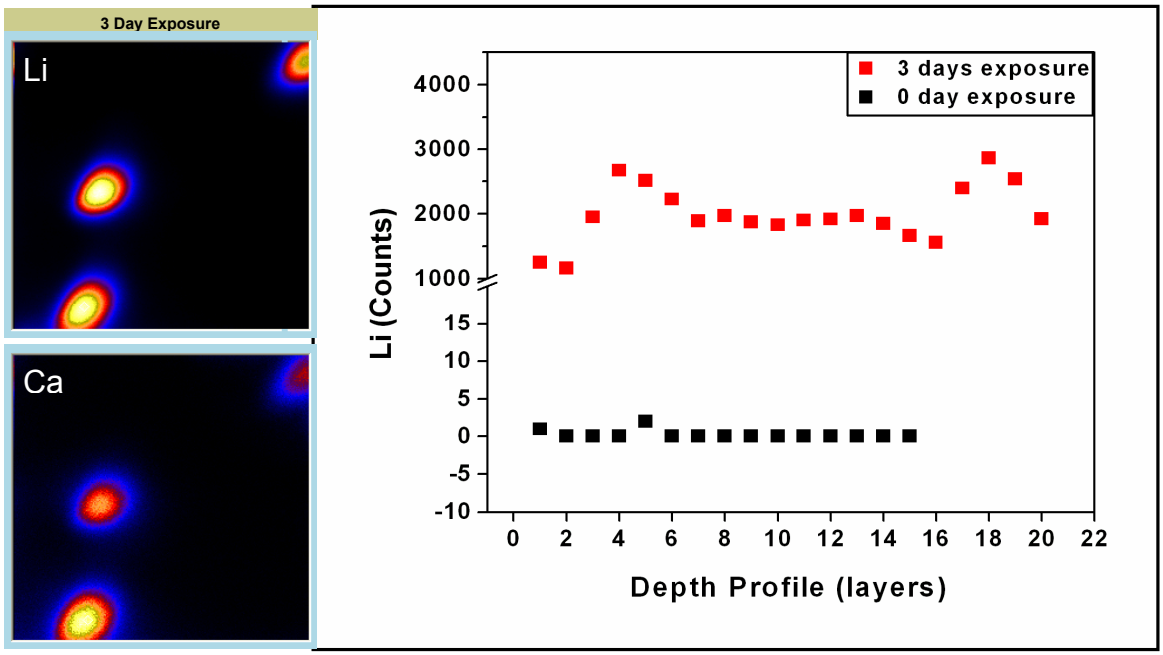

Fig. 15. Li profile in spore treated with LiF solution for 3 days compared to the control. Note break in scale. NanoSIMS ion images on the left show co-location of Li and Ca in the spores. This initial result suggests that hydration pathways provide a mechanism for short-time scale diffusion in/out of spores.

In the second set of experiments, fully hydrated spores were added to a dilute LiF solution for a series of time steps up to 3 days (Fig. 16). The data for these experiments demonstrate that Li uptake into the core is faster than 5 minutes, the shortest exposure time used for these experiments. This rate of diffusion into the spore is comparable to the rate of water diffusion into spores. Li content increases logarithmically, approaching the saturation level in 3 days. The level of Li in the spores reaches ~50% of the saturation value in ~1 day**.** The data indicate that at equilibrium, the spores will concentrate these elements by a factor of ~3 relative to the concentration of these elements in the solution.

Experiments with CsCl yielded similar results, but with higher variability that is likely because of the germinating effect of the chloride ion (Fig. 16). The relatively large difference between the ionic radii of Li and Cs (~0.7 angstroms for Li vs. ~2.2 angstroms for Cs) does not appear to be a factor in their uptake into the spore. This result is consistent with estimates that spore surfaces contain pores varying in diameter from 10 to 200 angstrom, which are large compared to either of these ions (Gerhardt & Black, 1961). These results support our model of high rates of elemental movement in and out of spores under fully hydrated conditions, with elemental binding being the primary control on changes in elemental abundance with time.

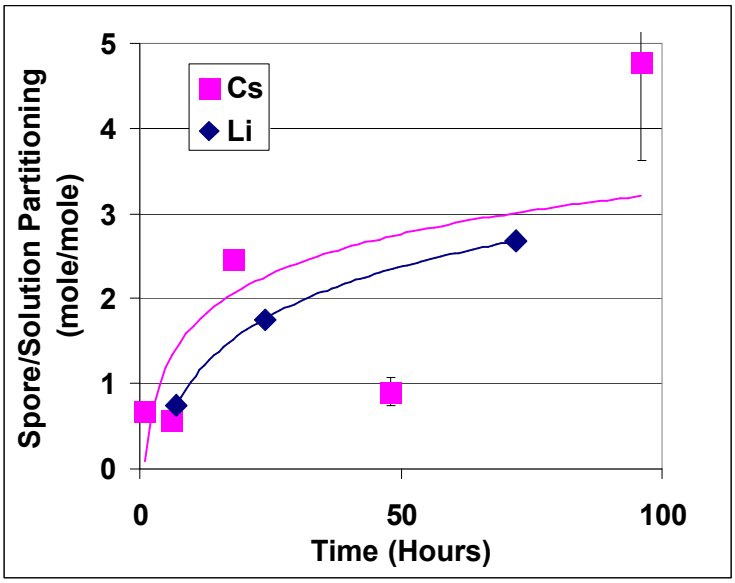

Fig. 16. Li and Cs spore/solution partitioning as a function of time of exposure to LiF or CsCl solution. Note that Li and Cs are concentrated in the spores relative to the solution.

Although the Li content of spores increases with time, the Li profiles within individual spores do not change significantly in form with time (Fig. 17). The spores maintain higher abundance of Li in the coat compared to the core for all time steps. The profiles do not show a steep gradient that flattens over time, which would indicate diffusion into the spore. The Cs profiles also show this consistent profile. These results are consistent with our results for water uptake into spores.

Taken together, these results suggest that under fully hydrated conditions diffusion of cations throughout the spore volume is rapid relative to the mechanism of cation incorporation into the spore. These results also suggest that the majority of the introduced cations that are not bound in the spore exit the spore with the bulk water

during dehydration. While some baseline level of introduced cation content (e.g., Li) may be residual, we hypothesize that the primary cause of increased levels of Li over time is increased binding within the spore through local diffusion and ion exchange. For a cation to become bound, it must reach a binding site and exchange with another cation, such as Na^+ or H^+. Under this model, the measured increase in cation content of the dried spore will primarily reflect the bound cations. The shape of the profile suggests that there is a higher abundance of binding sites in the coat, as compared to the core.

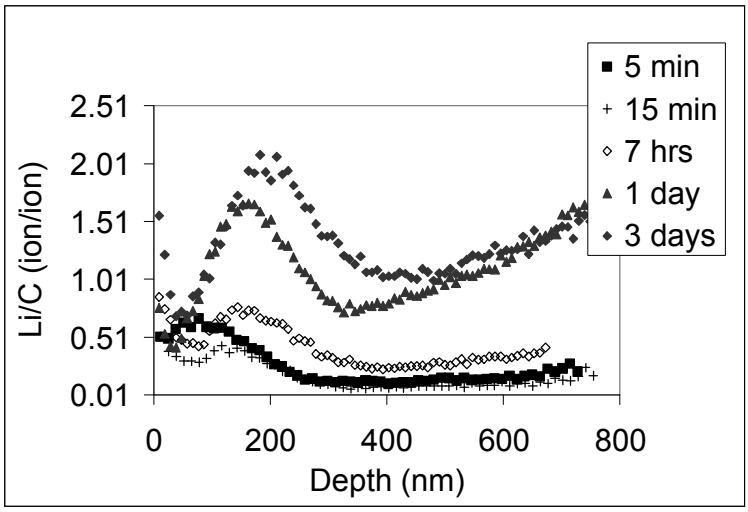

Fig. 17. Li/C profiles in spores treated with LiF solution for 5 minutes to 3 days.

For LiF, fluoride uptake is less significant than lithium uptake. This result is indicative of spores having greater affinity for cations than anions and is consistent with the primary available binding sites being negatively charged carboxyl, hydroxyl and amine groups. We hypothesize that charge balance is maintained by co-diffusion of Li^+ and F^- into the spore, exchange of Li^+ for another cation, and loss of F^- and the cation during dehydration. Uptake of chloride was also low in dormant spores, but the measurements were complicated by the fact that chloride stimulates germination. Fluoride does not stimulate spore germination.

We have performed anion leaching experiments to study the state of F and Cl in these spores (Fig. 18). Our results show difference in the mobility of F and Cl in the same experiment. F is leached from the spore core over time, whereas there is almost no change in core Cl levels under the same leach conditions. These results suggest that Cl is more tightly bound than F. We have not identified the binding sites.

In conclusion, we have clearly demonstrated the movement of ions (cations/anions) in spores in aqueous environment and thereby established diffusion as a likely contributor to the spore elemental signatures. Furthermore, our results suggest that in aqueous environment the rate of diffusion in spores is greater than the rate of exchange. Hence, the uptake of ions into spores in such an environment appears to be exchange limited. Also, for the range of ionic radii studied in our experiments the ionic radius does not appear to have a significant impact on the uptake mechanism.

In terms of developing spore chronometry, future experiments will focus on determining the rate of diffusion/exchange in spores under dehydrated and ambient

humidity conditions. We expect the rates to be slower under these conditions compared to an aqueous environment. Also, since ambient humidity conditions are typically variable it is necessary to determine the sensitivity of the diffusion rate to changes in relative humidity in order to develop a reliable diffusion based chronometer. In terms of the choice of ions, for future diffusion experiments we will focus on ionic species that are typically present in spores since they are the ones most relevant to the diffusion based spore chronometry.

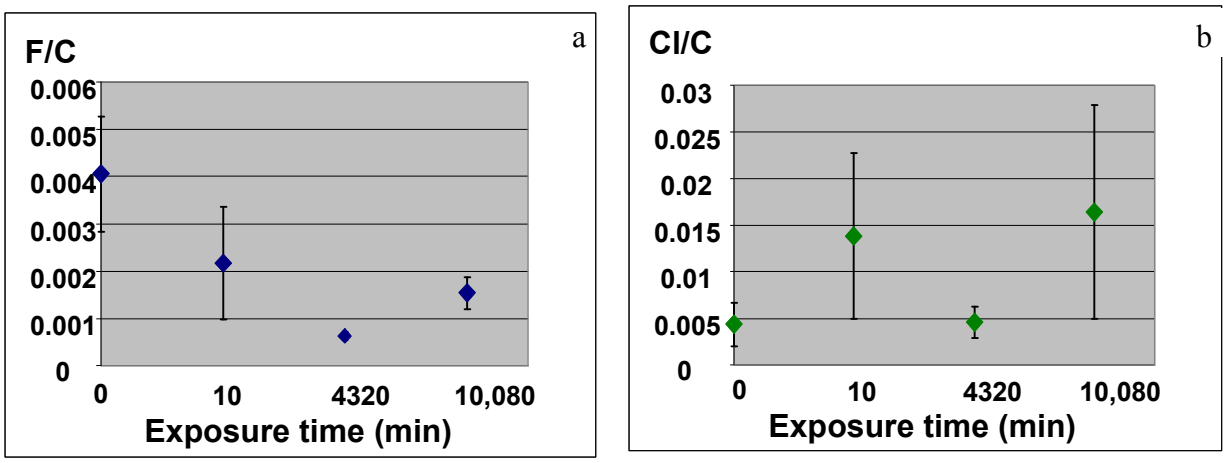

Fig. 18. (a) F/C and (b) Cl/C ratio in the core of control and milli-Q water treated spores. F content decreases with time, but Cl content does not change.

Exit Plan

Peter Weber has been asked to present results of our research to FBI senior scientists and Amerithrax agents, as well as to DHS and DTRA. The success of the project attracted funding from the FBI and DHS. Publications are in process.

Summary

Under this project, we have developed the necessary methods for characterizing spores by NanoSIMS, and we have conducted experiments and made measurements to understand the baseline controls on elemental uptake and distribution in spores. There are significant elemental gradients in the spores we have analyzed. These include gradients for biologically controlled elements, such as P, as well as gradients for elements such as Si, Cl and F, for which there is currently no generally accepted model for the controls on their distributions. In the majority of the samples we have examined, Si, Cl and F are associated with the spore margin. We have continued to study these elemental distributions under FBI and DHS funding. The capability that we have developed is broadening the national bioforensics capability, from basic characterization of spores to building the capability to gather forensic data from trace samples.

Acknowledgements

Katie Wheeler produced spore samples at CHORI. Stewart Fallon and Julie Smith assisted with NanoSIMS analyses. Christina Ramon performed ultramicrotomy and sample preparation. Giles Graham, Nick Teslich and Warren MoberlyChan performed FIB sectioning. Zurong Dai performed TEM imaging. Steve Velsko provided valuable guidance. Sasha Bajit provided multilayer samples for depth profile characterization. Larry Nittler provided software development support. This work was performed under the auspices of the U.S. Department of Energy by the University of California, Lawrence Livermore National Laboratory under Contract W-7405-Eng-4.

References

Blair, N. et al., 1985. Carbon isotopic fractionation in heterotrophic microbial metabolism. *Applied Environmental Microbiology*, 50: 996-1001.

Fein, J.B., S. Scott, N. Rivera, 2002. The effect of Fe on Si adsorption by *Bacillus subtilis* cell walls: insights into non-metabolic bacterial precipitation of silicate minerals. *Chemical Geology* **182**: 265-273.

Gerhardt, P., S. H. Black, 1961. Permeability of bacterial spores. *Journal of Bacteriology* **82**: 750-759.

Hortia, J. and Vass, A.A., 2003. Stable-isotope fingerprints of biological agents as forensic tools. *Journal of Forensic Sciences*, 48: 122-126.

Kent, A.J.R., Hutcheon, I.D., Ryerson, F.J. and Phinney, D.L., 2001. The temperature of formation of carbonate in martian meteorite ALH84001: constraints from cation diffusion. *Geochimica et Cosmochimica Acta*, 65: 311-321.

Kreuzer-Martin, H.W., Lott, M.J., Dorigan, J. and Ehleringer, J.R., 2003. Microbe forensics: Oxygen and hydrogen stable isotope ratios in *Bacillus subtilis* cells and spores. *Proceedings of the National Academy of Sciences*, 100: 815-819.

Peterson, B.J. and Fry, B., 1987. Stable isotopes in ecosystem studies. *Annual Review of Ecology and Systematics*, 18: 293-320.

Westphal, A.J., P.B. Price, T.J. Leighton, K.E. Wheeler, 2003. Kinetics of size changes of individual *Bacillus thuringiensis* spores in response to changes in relative humidity. *PNAS* **100**: 3463-3466.